
NEURAL PRUNING VIA GROWING REGULARIZATION

Huan Wang, Can Qin, Yulun Zhang, Yun Fu

Northeastern University, Boston, MA, USA

{wang.huan, qin.ca}@northeastern.edu,
yulun100@gmail.com, yunfu@ece.neu.edu

ABSTRACT

Regularization has long been utilized to learn sparsity in deep neural network pruning. However, its role is mainly explored in the small penalty strength regime. In this work, we extend its application to a new scenario where the regularization grows large gradually to tackle two central problems of pruning: pruning schedule and weight importance scoring. (1) The former topic is newly brought up in this work, which we find critical to the pruning performance while receives little research attention. Specifically, we propose an L_2 regularization variant with rising penalty factors and show it can bring significant accuracy gains compared with its one-shot counterpart, even when the *same* weights are removed. (2) The growing penalty scheme also brings us an approach to exploit the Hessian information for more accurate pruning *without knowing their specific values*, thus not bothered by the common Hessian approximation problems. Empirically, the proposed algorithms are easy to implement and scalable to large datasets and networks in *both structured and unstructured pruning*. Their effectiveness is demonstrated with modern deep neural networks on the CIFAR and ImageNet datasets, achieving competitive results compared to many state-of-the-art algorithms. Our code and trained models are publicly available at <https://github.com/mingsun-tse/regularization-pruning>.

1 INTRODUCTION

As deep neural networks advance in recent years LeCun et al. (2015); Schmidhuber (2015), their remarkable effectiveness comes at a cost of rising storage, memory footprint, computing resources and energy consumption Cheng et al. (2017); Deng et al. (2020). Neural network pruning Han et al. (2015; 2016); Li et al. (2017); Wen et al. (2016); He et al. (2017); Gale et al. (2019) is deemed as a promising force to alleviate this problem. Since its early debut Mozer & Smolensky (1989); Reed (1993), the central problem of neural network pruning has been (arguably) how to choose weights to discard, i.e., the weight importance scoring problem LeCun et al. (1990); Hassibi & Stork (1993); Molchanov et al. (2017b; 2019); Wang et al. (2019a); He et al. (2020).

The approaches to the scoring problem generally fall into two groups: importance-based and regularization-based Reed (1993). The former focuses on directly proposing certain theoretically sound importance criterion so that we can prune the unimportant weights once for all. Thus, the pruning process is typically one-shot. In contrast, regularization-based approaches typically select unimportant weights through training with a penalty term Han et al. (2015); Wen et al. (2016); Liu et al. (2017). However, the penalty strength is usually maintained in a small regime to avoid damaging the model expressivity. Whereas, a large penalty strength can be helpful, specifically in two aspects. (1) A large penalty can push unimportant weights rather close to zero, then the pruning later barely hurts the performance even if the simple weight magnitude is adopted as criterion. (2) It is well-known that different weights of a neural network lie on the regions with different local quadratic structures, i.e., Hessian information. Many methods try to tap into this to build a more accurate scoring LeCun et al. (1990); Hassibi & Stork (1993); Wang et al. (2019a); Singh & Alistarh (2020). However, for deep networks, it is especially hard to estimate Hessian. Sometimes, even the computing itself can be intractable without resorting to proper approximation Wang et al. (2019a). On this problem, we ask: *Is it possible to exploit the Hessian information without knowing their specific values?* This is the second scenario where a growing regularization can help. We will

show under a growing regularization, the weight magnitude will naturally separate because of their different underlying local quadratic structure, therein we can pick the unimportant weights more faithfully even using the simple magnitude-based criterion. Corresponding to these two aspects, we will present two algorithms based on a *growing L_2 regularization* paradigm, in which the first highlights a better pruning schedule¹ and the second explores a better pruning criterion.

Our contributions. (1) We propose a simple yet effective growing regularization scheme, which can help transfer the model expressivity to the remaining part during pruning. The encouraging performance inspires us that the pruning schedule may be as critical as the weight importance criterion and deserve more research attention. (2) We further adopt growing regularization to exploit Hessian implicitly, without knowing their specific values. The method can help choose the unimportant weights more faithfully with a theoretically sound basis. In this regard, our paper is the first to show the connection between magnitude-based pruning and Hessian-based pruning, pointing out that the latter can be turned into the first one through our proposed growing regularization scheme. (3) The proposed two algorithms are easy to implement and scalable to large-scale datasets and networks. We show their effectiveness compared with many state-of-the-arts. Especially, the methods can work seamlessly for both filter pruning and unstructured pruning.

2 RELATED WORK

Regularization-based pruning. The first group of relevant works is those applying regularization to learn sparsity. The most famous probably is to use L_0 or L_1 regularization [Louizos et al. \(2018\)](#); [Liu et al. \(2017\)](#); [Ye et al. \(2018\)](#) due to their sparsity-inducing nature. In addition, the common L_2 regularization is also explored for approximated sparsity [Han et al. \(2015; 2016\)](#). The early papers focus more on unstructured pruning, which is beneficial to model compression yet not to acceleration. For structured pruning in favor of acceleration, Group-wise Brain Damage [Lebedev & Lempitsky \(2016\)](#) and SSL [Wen et al. \(2016\)](#) propose to use Group LASSO [Yuan & Lin \(2006\)](#) to learn regular sparsity, where the penalty strength is still kept in small scale because the penalty is uniformly applied to all the weights. To resolve this, [Ding et al. \(2018\)](#) and [Wang et al. \(2019b\)](#) propose to employ different penalty factors for different weights, enabling large regularization.

Importance-based pruning. Importance-based pruning tries to establish certain advanced importance criteria that can reflect the true relative importance among weights as faithfully as possible. The pruned weights are usually decided immediately by some proposed formula instead of by training (although the whole pruning process can involve training, e.g., iterative pruning). The most widely used criterion is the magnitude-based: weight absolute value for unstructured pruning [Han et al. \(2015; 2016\)](#) or L_1/L_2 -norm for structured pruning [Li et al. \(2017\)](#). This heuristic criterion was proposed a long time ago [Reed \(1993\)](#) and has been argued to be inaccurate. In this respect, improvement mainly comes from using Hessian information to obtain a more accurate approximation of the increased loss when a weight is removed [LeCun et al. \(1990\)](#); [Hassibi & Stork \(1993\)](#). Hessian is intractable to compute for large networks, so some methods (e.g., EigenDamage [Wang et al. \(2019a\)](#), WoodFisher [Singh & Alistarh \(2020\)](#)) employ cheap approximation (such as K-FAC Fisher [Martens & Grosse \(2015\)](#)) to make the 2nd-order criteria tractable on deep networks.

Note that, there is no a hard boundary between the importance-based and regularization-based. Many papers present their schemes in the combination of the two [Ding et al. \(2018\)](#); [Wang et al. \(2019b\)](#). The difference mainly lies in their emphasis: Regularization-based method focuses more on an advanced penalty scheme so that the subsequent pruning criterion can be simple; while the importance-based one focus more on an advanced importance criterion itself. Meanwhile, regularization paradigm always involves iterative training, while the importance-based can be one-shot [LeCun et al. \(1990\)](#); [Hassibi & Stork \(1993\)](#); [Wang et al. \(2019a\)](#) (no training for picking weights to prune) or involve iterative training [Molchanov et al. \(2017b; 2019\)](#); [Ding et al. \(2019a;b\)](#).

Other model compression methods. Apart from pruning, there are also many other model compression approaches, e.g., quantization [Courbariaux & Bengio \(2016\)](#); [Courbariaux et al. \(2016\)](#); [Rastegari et al. \(2016\)](#), knowledge distillation [Buciluă et al. \(2006\)](#); [Hinton et al. \(2014\)](#), low-rank decomposition [Denton et al. \(2014\)](#); [Jaderberg et al. \(2014\)](#); [Lebedev et al. \(2014\)](#); [Zhang](#)

¹By pruning schedule, we mean the way to remove weights (e.g., removing all weights in a single step or multi-steps), *not* the training schedule such as learning rate settings, etc.

et al. (2015), and efficient architecture design or search Howard et al. (2017); Sandler et al. (2018); Howard et al. (2019); Zhang et al. (2018); Tan & Le (2019); Zoph & Le (2017); Elsken et al. (2019). They are orthogonal to network pruning and can work with the proposed methods to compress more.

3 PROPOSED METHOD

3.1 PROBLEM FORMULATION

Pruning can be formulated as a transformation $T(*)$ that takes a pretrained big model \mathbf{w} as input and output a small model \mathbf{w}_1 , typically followed by a fine-tuning process $F(*)$, which gives us the final output $\mathbf{w}_2 = F(\mathbf{w}_1)$. We do not focus on $F(*)$ since it is simply a standard neural network training process, but focus on the process of $\mathbf{w}_1 = T(\mathbf{w})$. The effect of pruning can be further specified into two sub-transformations: (1) $M = T_1(\mathbf{w})$, which obtains a binary mask vector M that decides which weights will be removed; (2) $T_2(\mathbf{w})$, which adjusts the values of remaining weights. That is,

$$\mathbf{w}_1 = T(\mathbf{w}) = T_1(\mathbf{w}) \odot T_2(\mathbf{w}) = M \odot T_2(\mathbf{w}). \quad (1)$$

For one-shot pruning, there is no iterative training at T_1 . It depends on a specific algorithm to decide whether to adjust the remaining weights. For example, OBD LeCun et al. (1990) and L_1 -norm pruning Li et al. (2017) do not adjust the kept weights (i.e., T_2 is the identity function) while OBS Hassibi & Stork (1993) does. For learning-based pruning, both T_1 and T_2 involve iterative training and the kept weights will always be adjusted.

In the following, we will present our algorithms in the **filter pruning** scenario since we mainly focus on model acceleration instead of compression in this work. Nevertheless, the methodology can seamlessly translate to the unstructured pruning case. The difference lies in how we define the *weight group*: For filter pruning, a 4-d tensor convolutional filter (or 2-d tensor for fully-connected layers) is regarded as a weight group, while for unstructured pruning, a single weight makes a group.

3.2 PRUNING SCHEDULE: GREG-1

Our first method (GReg-1) is a variant of L_1 -norm pruning Li et al. (2017). It obtains the mask M by L_1 -norm sorting but *adjusts the kept weights via regularization*. Specifically, given a pre-trained model \mathbf{w} and layer pruning ratio r_l , we sort the filters by L_1 -norm and set the mask to zero for those with the least norms. Then, unlike Li et al. (2017) which removes the unimportant weights *immediately* (i.e., one-shot fashion), we impose a growing L_2 penalty to drive them to zero first:

$$\lambda_j = \lambda_j + \delta\lambda, j \in \{j \mid M[j] = 0\}, \quad (2)$$

where λ_j is the penalty factor for j -th weight; $\delta\lambda$ is the granularity in which we add up the penalty. Clearly, a *smaller* $\delta\lambda$ means this regularization process *smoother*. Besides, λ_j is only updated every K_u iterations, which is a buffer time to let the network adapt to the new regularization. This algorithm is to explore whether the way we remove them (i.e., pruning schedule) leads to a difference given the *same* weights to prune. Simple as it is, the scheme can bring significant accuracy gains especially under a large pruning ratio (Tab. 1). Note that, we intentionally set $\delta\lambda$ the *same* for all the unimportant weights to keep the core idea simple. Natural extensions of using different penalty factors for different weights (such as those in Ding et al. (2018); Wang et al. (2019b)) may be worth exploring but out of the scope of this work.

When λ_j reaches a pre-set ceiling τ , we terminate the training and prune those with the least L_1 -norms, then fine-tune. Notably, the pruning will *barely* hurt the accuracy since the unimportant weights have been compressed to typically less than $\frac{1}{1000}$ the magnitude of remaining weights.

3.3 IMPORTANCE CRITERION: GREG-2

Our second algorithm is to further take advantage of the growing regularization scheme, not for pruning schedule but scoring. The training of neural networks is prone to overfitting, so regularization is normally employed. L_2 regularization (or referred to as weight decay) is a standard technique for deep network training. Given a dataset \mathcal{D} , model parameters \mathbf{w} , the total loss will typically be

$$\mathcal{E}(\mathbf{w}, \mathcal{D}) = \mathcal{L}(\mathbf{w}, \mathcal{D}) + \frac{1}{2}\lambda\|\mathbf{w}\|_2^2, \quad (3)$$

where \mathcal{L} is the task loss function. When the training converges, there should be

$$\lambda w_i^* + \frac{\partial \mathcal{L}}{\partial w_i} \Big|_{w_i=w_i^*} = 0, \quad (4)$$

where w_i^* indicates the i -th weight *at its local minimum*. Eq. (4) shows that, for each specific weight element, its equilibrium position is determined by two forces: loss gradient (i.e., guidance from the task) and regularization gradient (i.e., guidance from our prior). Our idea is to slightly increase the λ to break the equilibrium and see how it results in a new one. A general impression is: If λ goes a little higher, the penalty force will drive the weights further towards origin and it will not stop unless proper loss gradient comes to halt it and then a new equilibrium is reached at \hat{w}_i^* . Considering different weights have different scales, we define a ratio $r_i = \hat{w}_i^*/w_i^*$ to describe how much the weight magnitude changes after increasing the penalty factor. Our interest lies in how the r_i differs from one another and how it relates to the underlying Hessian information.

Deep neural networks are well-known over-parameterized and highly non-convex. To obtain a feasible analysis, we adopt a local quadratic approximation of the loss function based on Taylor series expansion [Strang \(1991\)](#) following common practices [LeCun et al. \(1990\)](#); [Hassibi & Stork \(1993\)](#); [Wang et al. \(2019a\)](#). Then when the model is converged, the error \mathcal{E} can be described by the converged weights \mathbf{w}^* and the underlying Hessian matrix \mathbf{H} (note \mathbf{H} is p.s.d. since the model is converged). After increasing the penalty λ by $\delta\lambda$, the new converged weights can be proved to be

$$\hat{\mathbf{w}}^* = (\mathbf{H} + \delta\lambda \mathbf{I})^{-1} \mathbf{H} \mathbf{w}^*, \quad (5)$$

where \mathbf{I} stands for the identity matrix. Here we meet with the common problem of estimating Hessian and its inverse, which are well-known to be intractable for deep neural networks. We explore two simplified cases to help us move forward.

(1) \mathbf{H} is diagonal, which is a common simplification for Hessian [LeCun et al. \(1990\)](#), implying that the weights are independent of each other. For w_i^* with second derivative h_{ii} . With L_2 penalty increased by $\delta\lambda$ ($\delta\lambda > 0$), the new converged weights can be proved to be

$$\hat{w}_i^* = \frac{h_{ii}}{h_{ii} + \delta\lambda} w_i^*, \Rightarrow r_i = \frac{\hat{w}_i^*}{w_i^*} = \frac{1}{\delta\lambda/h_{ii} + 1}, \quad (6)$$

where $r_i \in [0, 1)$ since $h_{ii} \geq 0$ and $\delta\lambda > 0$. As seen, **larger h_{ii} results in larger r_i (closer to 1), meaning that the weight is relatively less moved towards the origin**. Our second algorithm primarily builds upon this finding, which implies when we add a penalty perturbation to the converged network, the way that different weights respond can reflect their underlying Hessian information.

(2) In practice, we know \mathbf{H} is rarely diagonal. How the dependency among weights affects the finding above is of interest. To have a closed form of inverse Hessian in Eq. (5), we explore the 2-d case, namely, $\mathbf{w}^* = \begin{pmatrix} w_1^* \\ w_2^* \end{pmatrix}$, $\mathbf{H} = \begin{pmatrix} h_{11} & h_{12} \\ h_{12} & h_{22} \end{pmatrix}$, $\hat{\mathbf{H}} = \begin{pmatrix} h_{11} + \delta\lambda & h_{12} \\ h_{12} & h_{22} + \delta\lambda \end{pmatrix}$. The new converged weights can be analytically solved below, where the approximation equality is because that $\delta\lambda$ is rather small,

$$\begin{Bmatrix} \hat{w}_1^* \\ \hat{w}_2^* \end{Bmatrix} = \frac{1}{|\hat{\mathbf{H}}|} \begin{Bmatrix} (h_{11}h_{22} + h_{11}\delta\lambda - h_{12}^2)w_1^* + \delta\lambda h_{12}w_2^* \\ (h_{11}h_{22} + h_{22}\delta\lambda - h_{12}^2)w_2^* + \delta\lambda h_{12}w_1^* \end{Bmatrix} \approx \frac{1}{|\hat{\mathbf{H}}|} \begin{Bmatrix} (h_{11}h_{22} + h_{11}\delta\lambda - h_{12}^2)w_1^* \\ (h_{11}h_{22} + h_{22}\delta\lambda - h_{12}^2)w_2^* \end{Bmatrix}, \quad (7)$$

$$\Rightarrow r_1 = \frac{1}{|\hat{\mathbf{H}}|} (h_{11}h_{22} + h_{11}\delta\lambda - h_{12}^2), \quad r_2 = \frac{1}{|\hat{\mathbf{H}}|} (h_{11}h_{22} + h_{22}\delta\lambda - h_{12}^2). \quad (8)$$

As seen, $h_{11} > h_{22}$ also leads to $r_1 > r_2$, in line with the finding above. The existence of weight dependency (i.e., the h_{12}) actually does *not* affect the conclusion since it is included in both ratios.

These theoretical analyses show us that when the penalty is increased at the same pace, because of different local curvature structures, the weights actually respond differently – weights with **larger** curvature will be **less** moved. As such, the magnitude discrepancy among weights will be magnified as λ grows. Ultimately, the weights will naturally separate (see Fig. 1 for an empirical validation). When the discrepancy is large enough, even the simple L_1 -norm can make an accurate criterion. Notably, the whole process happens itself with the uniformly rising L_2 penalty, *no need to know the Hessian values*, thus not bothered by any issue arising from Hessian approximation in relevant prior arts [LeCun et al. \(1990\)](#); [Hassibi & Stork \(1993\)](#); [Wang et al. \(2019a\)](#); [Singh & Alistarh \(2020\)](#).

In terms of the specific algorithm, *all* the penalty factor is increased at the same pace,

$$\lambda_j = \lambda_j + \delta\lambda, \text{ for all } j. \quad (9)$$

Algorithm 1 GReg-1 and GReg-2 Algorithms

- 1: **Input:** Pre-trained model \mathbf{w} , pruning ratio for l -th layer $r_l, l = 1 \sim L$, original weight decay γ .
 - 2: **Input:** Regularization ceiling τ , **ceiling for picking** τ' , interval K_u, K_s , granularity $\delta\lambda$.
 - 3: **Init:** Iteration $i = 0$. $\lambda_j = 0$ for all filter j . **Set kept filter indexes** S_l^k to \emptyset for each layer l .
 - 4: **Init:** **Set pruned filter indexes** S_l^p by L_1 -norm sorting, **set** S_l^p to full set, for each layer l .
 - 5: **while** $\lambda_j \leq \tau, j \in S_l^p$ **do**
 - 6: **if** $i \% K_u = 0$ **then**
 - 7: **if** $S_l^k = \emptyset$ and $\lambda_j > \tau', j \in S_l^p$ **then**
 - 8: **Set** S_l^p by L_1 -norm scoring, S_l^k as the complementary set of S_l^p , for each layer l .
 - 9: **end if**
 - 10: $\lambda_j = \lambda_j + \delta\lambda$ for $j \in S_l^p$, $\lambda_j = -\gamma$ for $j \in S_l^k$, for each layer l
 - 11: **end if**
 - 12: Weight update by stochastic gradient descent (where the regularization is enforced).
 - 13: $i = i + 1$.
 - 14: **end while**
 - 15: Train for another K_s iterations to stabilize. Then prune by L_1 -norms and get model \mathbf{w}_1 .
 - 16: Fine-tune \mathbf{w}_1 to regain accuracy.
 - 17: **Output:** Pruned model \mathbf{w}_2 .
-

When λ_j reaches some ceiling τ' , the magnitude gap turns large enough to let L_1 -norm do scoring faithfully. After this, the procedures are similar to those in GReg-1: λ for the unimportant weights are further increased. One extra step is to bring back the kept weights to the normal magnitude. Although they are the “survivors” during the previous competition under a large penalty, their expressivity are also hurt. To be exact, we adopt *negative* penalty factor for the kept weights to encourage them to recover. When the λ for unimportant weights reaches the threshold τ (akin to that of GReg-1), the training is terminated. L_1 -pruning is conducted and then fine-tune to regain accuracy. To this end, the proposed two algorithms can be summarized in Algorithm 1.

Pruning ratios. We employ *pre-specified* pruning ratios in this work to keep the core method neat (see Appendix for more discussion). Exploring layer-wise sensitivity is out of the scope of this work, but clearly any method that finds more proper pruning ratios can readily work with our approaches.

4 EXPERIMENTAL RESULTS

Datasets and networks. We first conduct analyses on the CIFAR10/100 datasets Krizhevsky (2009) with ResNet56 He et al. (2016)/VGG19 Simonyan & Zisserman (2015). Then we evaluate our methods on the large-scale ImageNet dataset Deng et al. (2009) with ResNet34 and 50 He et al. (2016). For CIFAR datasets, we train our baseline models with accuracies comparable to those in the original papers. For ImageNet, we take the official PyTorch Paszke et al. (2019) pre-trained models² as baseline to maintain comparability with other methods.

Training settings. To control the irrelevant factors as we can, for comparison methods that release their pruning ratios, we will adopt their ratios; otherwise, we will use our specified ones. We compare the speedup (measured by FLOPs reduction) since we mainly target model acceleration rather than compression. Detailed training settings (e.g., hyper-parameters and layer pruning ratios) are summarized in the Appendix. *Our code and trained models will be made available to the public.*

4.1 RESNET56/VGG19 ON CIFAR-10/100

Pruning schedule: GReg-1. First, we explore the effect of different pruning schedules on the performance of pruning. Specifically, we conduct two sets of experiments for comparison: (1) prune by L_1 -norm sorting and fine-tune Li et al. (2017) (shorted as “ L_1 +one-shot”); (2) employ the proposed growing regularization scheme (“GReg-1”) and fine-tune. We use a uniform pruning ratio scheme here: Pruning ratio r is the *same* for all l -th conv layer (the first layer is *not* pruned following common practice Gale et al. (2019)). For ResNet56, since it has the residual addition restriction, we only prune the first conv layer in a block as previous works do Li et al. (2017). For comprehensive

²<https://pytorch.org/docs/stable/torchvision/models.html>

Table 1: Comparison between pruning schedules: one-shot pruning vs. our proposed GReg-1. Each setting is randomly run for 3 times, mean and std accuracies reported.

| ResNet56 + CIFAR10: Baseline accuracy 93.36%, #Params: 0.85M, FLOPs: 0.25G | | | | | |
|--|-------------------------|-------------------------|-------------------------|-------------------------|-------------------------|
| Pruning ratio r (%) | 50 | 70 | 90 | 92.5 | 95 |
| Sparsity (%) / Speedup | 49.82/1.99 \times | 70.57/3.59 \times | 90.39/11.41 \times | 93.43/14.76 \times | 95.19/19.31 \times |
| Acc. (%), L_1 +one-shot | 92.97 \pm 0.15 | 91.88 \pm 0.09 | 87.34 \pm 0.21 | 87.31 \pm 0.28 | 82.79 \pm 0.22 |
| Acc. (%), GReg-1, ours | 93.06 \pm 0.09 | 92.23 \pm 0.21 | 89.49 \pm 0.23 | 88.39 \pm 0.15 | 85.97 \pm 0.16 |
| Acc. gain (%) | 0.09 | 0.35 | 2.15 | 1.08 | 3.18 |
| VGG19 + CIFAR100: Baseline accuracy 74.02%, #Params: 20.08M, FLOPs: 0.80G | | | | | |
| Pruning ratio r (%) | 50 | 60 | 70 | 80 | 90 |
| Sparsity (%) / Speedup | 74.87/3.60 \times | 84.00/5.41 \times | 90.98/8.84 \times | 95.95/17.30 \times | 98.96/44.22 \times |
| Acc. (%), L_1 +one-shot | 71.49 \pm 0.14 | 70.27 \pm 0.12 | 66.05 \pm 0.04 | 61.59 \pm 0.03 | 51.36 \pm 0.11 |
| Acc. (%), GReg-1, ours | 71.50 \pm 0.12 | 70.33 \pm 0.12 | 67.35 \pm 0.15 | 63.55 \pm 0.29 | 57.09 \pm 0.03 |
| Acc. gain (%) | 0.01 | 0.06 | 1.30 | 1.96 | 5.73 |

comparisons, the pruning ratios vary in a large spectrum, covering acceleration ratios from around $2\times$ to $44\times$. Note that we do not intend to obtain the best performance here but systematically explore the effect of different pruning schedules, so we employ relatively simple settings (e.g., the uniform pruning ratios). For fair comparisons, the fine-tuning scheme (e.g., number of epochs, learning rate schedule, etc.) is *the same* for different methods. Therefore, the key comparison here is to see which method can deliver a better base model before fine-tuning.

The results are shown in Tab. 1. We have the following observations: (1) On the whole, the proposed GReg-1 *consistently* outperforms L_1 +one-shot. It is important to reiterate that the two settings have *exactly the same* pruned weights, so the only difference is how they are removed. The accuracy gaps show that apart from importance scoring, pruning schedule is also a critical factor. In the Appendix, we will present more results to demonstrate this finding actually is *general*, not merely limited to the case of L_1 -norm criterion. The proposed regularization-based pruning schedule is consistently more favorable than the one-shot counterpart. (2) The larger pruning ratio, the more pronounced of the gain. This is reasonable since when more weights are pruned, the network cannot recover by its inherent plasticity [Mittal et al. \(2018\)](#), then the regularization-based way is more helpful because it helps the model transfer its expressive power to the remaining part. When the pruning ratio is relatively small (such as ResNet56, $r = 50\%$), the plasticity of the model is enough to heal, so the benefit from GReg-1 is less significant compared with the one-shot counterpart.

Importance criterion: GReg-2. Here we empirically validate our finding in Sec. 3.3, that is, with uniformly rising L_2 penalty, the weights should naturally separate. In Fig. 1 (Row 1), we plot the standard deviation (divided by the means for normalization since the magnitude varies over iterations) of filter L_1 -norms as the regularization grows. As seen, the normalized L_1 -norm stdev grows larger and larger as λ grows. This phenomenon *consistently* appears across different models and datasets. To figuratively understand how the increasing penalty affects the relative magnitude over time, in Fig. 1 (Row 2), we plot the relative L_1 -norms (divided by the max L_1 -norm for normalization) at different iterations. As shown, it is hard to tell which filters are really important by the initial filter magnitude (Iter 0), but under a large penalty later, their discrepancy turns more and more obvious and finally it is very easy to identify which filters are more important. Since the magnitude gap is so large, the simple L_1 -norm can make a sufficiently faithful criterion.

CIFAR benchmarks. Finally, we compare the proposed algorithms with existing methods on the CIFAR datasets (Tab. 2). Here we adopt non-uniform pruning ratios (see the Appendix for specific numbers) for the best accuracy-FLOPs trade-off. On CIFAR10, compared with AMC [He et al. \(2018b\)](#), though it adopts better layer-wise pruning ratios via reinforcement-learning, our algorithms can still deliver more favorable performance using sub-optimal human-specified ratios. AFP [Ding et al. \(2018\)](#) is another work exploring large regularization, while they do not adopt the *growing* scheme as we do. Its performance is also less favorable on CIFAR10 as shown in the table. Although our methods perform a little worse than C-SGD [Ding et al. \(2019a\)](#) on CIFAR10, on the large-scale ImageNet dataset, we will show our methods are significantly better than C-SGD.

Notably, on CIFAR100, Kron-OBD/OBS (an extension by [Wang et al. \(2019a\)](#) of the original OBD/OBS from unstructured pruning to structured pruning) are believed to be more accurate than

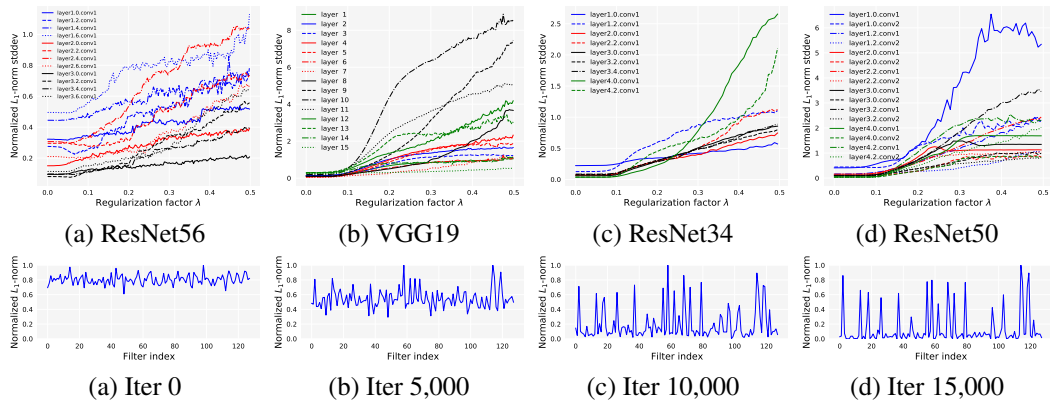


Figure 1: Row 1: Illustration of weight separation as L_2 penalty grows. Row 2: Normalized filter L_1 -norm over iterations for ResNet50 layer2.3.conv1 (please see the Appendix for VGG19 plots).

Table 2: Comparison of different methods on the CIFAR10 and CIFAR100 datasets.

| Method | Network/Dataset | Base acc. (%) | Pruned acc. (%) | Acc. drop | Speedup |
|---------------------------------|------------------|---------------|-----------------|--------------|---------------|
| CP He et al. (2017) | ResNet56/CIFAR10 | 92.80 | 91.80 | 1.00 | 2.00× |
| AMC He et al. (2018b) | | 92.80 | 91.90 | 0.90 | 2.00× |
| SFP He et al. (2018a) | | 93.59 | 93.36 | 0.23 | 2.11× |
| AFP Ding et al. (2018) | | 93.93 | 92.94 | 0.99 | 2.56 × |
| C-SGD Ding et al. (2019a) | | 93.39 | 93.44 | -0.05 | 2.55× |
| GReg-1 (ours) | | 93.36 | 93.18 | 0.18 | 2.55× |
| GReg-2 (ours) | 93.36 | 93.36 | 0.00 | 2.55× | |
| Kron-OBDD Wang et al. (2019a) | VGG19/CIFAR100 | 73.34 | 60.70 | 12.64 | 5.73× |
| Kron-OBS Wang et al. (2019a) | | 73.34 | 60.66 | 12.68 | 6.09× |
| EigenDamage Wang et al. (2019a) | | 73.34 | 65.18 | 8.16 | 8.80× |
| GReg-1 (ours) | | 74.02 | 67.55 | 6.67 | 8.84 × |
| GReg-2 (ours) | | 74.02 | 67.75 | 6.47 | 8.84 × |

L_1 -norm in terms of capturing relative weight importance LeCun et al. (1990); Hassibi & Stork (1993); Wang et al. (2019a). Yet, they are significantly outperformed by our GReg-1 based on the simple L_1 -norm scoring. This may inspire us that an average pruning schedule (like the one-shot fashion) can offset the gain from a more advanced importance scoring scheme.

4.2 RESNET34/50 ON IMAGENET

Then we evaluate our methods on the standard large-scale ImageNet benchmarks with ResNets He et al. (2016). We refer to the official PyTorch ImageNet training example³ to make sure the implementation (such as data augmentation, weight decay, momentum, etc.) is standard. Please refer to the summarized training setting in the Appendix for details.

The results are shown in Tab. 3. Methods with similar speedup are grouped together for easy comparison. In general, our method achieves comparable or better performance across various speedups on ResNet34 and 50. Concretely, (1) On both ResNet34 and 50, when the speedup is small (less than 2×), only our methods (and AOFD Ding et al. (2019b) for ResNet50) can even *improve* the top-1 accuracy. This phenomenon is broadly found by previous works Wen et al. (2016); Wang et al. (2018); He et al. (2017) but mainly on small datasets like CIFAR, while we make it on the much challenging ImageNet benchmark. (2) Similar to the results on CIFAR (Tab. 1), when the speedup is larger, the advantage of our method is more obvious. For example, ours GReg-2 only outperforms Taylor-FO Molchanov et al. (2019) by 0.86% top-1 accuracy at the $\sim 2\times$ setting, while at $\sim 3\times$, GReg-2 is better by 2.21% top-1 accuracy. (3) Many methods work on the weight importance criterion problem, including some very recent ones (ProvableFP Liebenwein et al. (2020), LFPC He et al. (2020)). Yet as shown, our simple variant of L_1 -norm pruning can still be a strong competitor in

³<https://github.com/pytorch/examples/tree/master/imagenet>

Table 3: Acceleration comparison on ImageNet. FLOPs: ResNet34: 3.66G, ResNet50: 4.09G.

| Method | Network | Base top-1 (%) | Pruned top-1 (%) | Top-1 drop | Speedup | |
|---|----------|----------------|------------------|--------------|----------------------|----------------------|
| L_1 (pruned-B) Li et al. (2017) | ResNet34 | 73.23 | 72.17 | 0.06 | 1.32 \times | |
| Taylor-FO Molchanov et al. (2019) | | 73.31 | 72.83 | 0.48 | 1.29 \times | |
| GReg-1 (ours) | | 73.31 | 73.54 | -0.23 | 1.32 \times | |
| GReg-2 (ours) | | 73.31 | 73.61 | -0.30 | 1.32 \times | |
| ProvableFP Liebenwein et al. (2020) | ResNet50 | 76.13 | 75.21 | 0.92 | 1.43 \times | |
| GReg-1 (ours) | | 76.13 | 76.27 | -0.14 | 1.49 \times | |
| AOFP Ding et al. (2019b) | ResNet50 | 75.34 | 75.63 | -0.29 | 1.49 \times | |
| GReg-2 (ours)* | | 75.40 | 76.13 | -0.73 | 1.49 \times | |
| SFP He et al. (2018a) | ResNet50 | 76.15 | 74.61 | 1.54 | 1.72 \times | |
| HRank Lin et al. (2020a) | | 76.15 | 74.98 | 1.17 | 1.78 \times | |
| Taylor-FO Molchanov et al. (2019) | | 76.18 | 74.50 | 1.68 | 1.82 \times | |
| Factorized Li et al. (2019) | | 76.15 | 74.55 | 1.60 | 2.33 \times | |
| DCP Zhuang et al. (2018) | | 76.01 | 74.95 | 1.06 | 2.25 \times | |
| CCP-AC Peng et al. (2019) | | 76.15 | 75.32 | 0.83 | 2.18 \times | |
| GReg-1 (ours) | | 76.13 | 75.16 | 0.97 | 2.31 \times | |
| GReg-2 (ours) | | 76.13 | 75.36 | 0.77 | 2.31 \times | |
| C-SGD-50 Ding et al. (2019a) | | ResNet50 | 75.34 | 74.54 | 0.80 | 2.26 \times |
| AOFP Ding et al. (2019b) | | | 75.34 | 75.11 | 0.23 | 2.31 \times |
| GReg-2 (ours)* | | | 75.40 | 75.22 | 0.18 | 2.31 \times |
| LFPC He et al. (2020) | | ResNet50 | 76.15 | 74.46 | 1.69 | 2.55 \times |
| GReg-1 (ours) | | | 76.13 | 74.85 | 1.28 | 2.56 \times |
| GReg-2 (ours) | | | 76.13 | 74.93 | 1.20 | 2.56 \times |
| Taylor-FO Molchanov et al. (2019) | 76.18 | | 71.69 | 4.49 | 3.05 \times | |
| GReg-1 (ours) | ResNet50 | 76.13 | 73.75 | 2.38 | 3.06 \times | |
| GReg-2 (ours) | | 76.13 | 73.90 | 2.23 | 3.06 \times | |

* Since the base models of C-SGD and AOFP have a much lower accuracy than ours, for fair comparison, we train our own base models with similar accuracy.

Table 4: Compression comparison on ImageNet with ResNet50. #Parameters: 25.56M.

| Method | Base top-1 (%) | Pruned top-1 (%) | Top-1 drop | Sparsity (%) |
|--|----------------|------------------|-------------|--------------|
| GSM Ding et al. (2019c) | 75.72 | 74.30 | 1.42 | 80.00 |
| Variational Dropout Molchanov et al. (2017a) | 76.69 | 75.28 | 1.41 | 80.00 |
| DPF Lin et al. (2020b) | 75.95 | 74.55 | 1.40 | 82.60 |
| WoodFisher Singh & Alistarh (2020) | 75.98 | 75.20 | 0.78 | 82.70 |
| GReg-1 (ours) | 76.13 | 75.45 | 0.68 | 82.70 |
| GReg-2 (ours) | 76.13 | 75.27 | 0.86 | 82.70 |

terms of accuracy-FLOPs trade-off. This reiterates one of our key ideas in this work that the pruning schedule may be as important as weight importance scoring and worth more research attention.

Unstructured pruning. Although we mainly target filter pruning in this work, the proposed methods actually can be applied to unstructured pruning as effectively. In Tab. 4, we present the results of unstructured pruning on ResNet50. WoodFisher [Singh & Alistarh \(2020\)](#) is the state-of-the-art Hessian-based unstructured pruning approach. Notably, without any Hessian approximation, our GReg-2 can achieve comparable performance with it (better absolute accuracy, yet slightly worse accuracy drop). Besides, the simple magnitude pruning variant GReg-1 delivers more favorable result, implying that a better pruning schedule also matters in the unstructured pruning case.

5 CONCLUSION

Regularization is long deemed as a sparsity-learning tool in neural network pruning, which usually works in the small strength regime. In this work, we present two algorithms that exploit regularization in a new fashion that the penalty factor is uniformly raised to a large level. Two central problems regarding deep neural pruning are tackled by the proposed methods, pruning schedule and weight importance criterion. The proposed approaches rely on few impractical assumptions, have a sound theoretical basis, and are scalable to large datasets and networks. Apart from the methodology itself, the encouraging results on CIFAR and ImageNet also justify our general ideas in this paper: (1)

In addition to weight importance scoring, pruning schedule is another pivotal factor in deep neural pruning which may deserve more research attention. (2) Without any Hessian approximation, we can still tap into its power for pruning with the help of growing L_2 regularization.

REFERENCES

- Cristian Buciluă, Rich Caruana, and Alexandru Niculescu-Mizil. Model compression. In *SIGKDD*, 2006. 2
- Yu Cheng, Duo Wang, Pan Zhou, and Tao Zhang. A survey of model compression and acceleration for deep neural networks. *arXiv preprint arXiv:1710.09282*, 2017. 1
- M. Courbariaux and Y. Bengio. BinaryNet: Training deep neural networks with weights and activations constrained to +1 or -1. *arXiv preprint arXiv:1602.02830*, 2016. 2
- Matthieu Courbariaux, Itay Hubara, Daniel Soudry, Ran El-Yaniv, and Yoshua Bengio. Binarized neural networks: Training deep neural networks with weights and activations constrained to +1 or -1. *arXiv preprint arXiv:1602.02830*, 2016. 2
- Jia Deng, Wei Dong, Richard Socher, Li-Jia Li, Kai Li, and Li Fei-Fei. Imagenet: A large-scale hierarchical image database. In *CVPR*, 2009. 5
- Lei Deng, Guoqi Li, Song Han, Luping Shi, and Yuan Xie. Model compression and hardware acceleration for neural networks: A comprehensive survey. *Proceedings of the IEEE*, 108(4): 485–532, 2020. 1
- Emily L Denton, Wojciech Zaremba, Joan Bruna, Yann LeCun, and Rob Fergus. Exploiting linear structure within convolutional networks for efficient evaluation. In *NeurIPS*, 2014. 2
- Xiaohan Ding, Guiguang Ding, Jungong Han, and Sheng Tang. Auto-balanced filter pruning for efficient convolutional neural networks. In *AAAI*, 2018. 2, 3, 6, 7
- Xiaohan Ding, Guiguang Ding, Yuchen Guo, and Jungong Han. Centripetal sgd for pruning very deep convolutional networks with complicated structure. In *CVPR*, 2019a. 2, 6, 7, 8
- Xiaohan Ding, Guiguang Ding, Yuchen Guo, Jungong Han, and Chenggang Yan. Approximated oracle filter pruning for destructive cnn width optimization. In *ICML*, 2019b. 2, 7, 8, 12
- Xiaohan Ding, Xiangxin Zhou, Yuchen Guo, Jungong Han, Ji Liu, et al. Global sparse momentum sgd for pruning very deep neural networks. In *NeurIPS*, 2019c. 8
- Thomas Elsken, Jan Hendrik Metzen, and Frank Hutter. Neural architecture search: A survey. *JMLR*, 20(55):1–21, 2019. 3
- Trevor Gale, Erich Elsen, and Sara Hooker. The state of sparsity in deep neural networks. *arXiv preprint arXiv:1902.09574*, 2019. 1, 5
- Song Han, Jeff Pool, John Tran, and William J Dally. Learning both weights and connections for efficient neural network. In *NeurIPS*, 2015. 1, 2
- Song Han, Huizi Mao, and William J Dally. Deep compression: Compressing deep neural networks with pruning, trained quantization and huffman coding. In *ICLR*, 2016. 1, 2
- B. Hassibi and D. G. Stork. Second order derivatives for network pruning: Optimal brain surgeon. In *NeurIPS*, 1993. 1, 2, 3, 4, 7
- K. He, X. Zhang, S. Ren, and J. Sun. Deep residual learning for image recognition. In *CVPR*, 2016. 5, 7
- Yang He, Guoliang Kang, Xuanyi Dong, Yanwei Fu, and Yi Yang. Soft filter pruning for accelerating deep convolutional neural networks. In *IJCAI*, 2018a. 7, 8
- Yang He, Yuhang Ding, Ping Liu, Linchao Zhu, Hanwang Zhang, and Yi Yang. Learning filter pruning criteria for deep convolutional neural networks acceleration. In *CVPR*, 2020. 1, 7, 8

-
- Yihui He, Xiangyu Zhang, and Jian Sun. Channel pruning for accelerating very deep neural networks. In *ICCV*, 2017. 1, 7, 12
- Yihui He, Ji Lin, Zhijian Liu, Hanrui Wang, Li-Jia Li, and Song Han. AMC: Automl for model compression and acceleration on mobile devices. In *ECCV*, 2018b. 6, 7
- Geoffrey Hinton, Oriol Vinyals, and Jeff Dean. Distilling the knowledge in a neural network. In *NeurIPS Workshop*, 2014. 2
- Andrew Howard, Mark Sandler, Grace Chu, Liang-Chieh Chen, Bo Chen, Mingxing Tan, Weijun Wang, Yukun Zhu, Ruoming Pang, Vijay Vasudevan, et al. Searching for mobilenetv3. *arXiv preprint arXiv:1905.02244*, 2019. 3
- Andrew G Howard, Menglong Zhu, Bo Chen, Dmitry Kalenichenko, Weijun Wang, Tobias Weyand, Marco Andreetto, and Hartwig Adam. Mobilenets: Efficient convolutional neural networks for mobile vision applications. *arXiv preprint arXiv:1704.04861*, 2017. 3
- Max Jaderberg, Andrea Vedaldi, and Andrew Zisserman. Speeding up convolutional neural networks with low rank expansions. In *BMVC*, 2014. 2
- Alex Krizhevsky. Learning multiple layers of features from tiny images. Technical report, Citeseer, 2009. 5
- V. Lebedev and V. Lempitsky. Fast convnets using group-wise brain damage. In *CVPR*, 2016. 2
- Vadim Lebedev, Yaroslav Ganin, Maksim Rakhuba, Ivan Oseledets, and Victor Lempitsky. Speeding-up convolutional neural networks using fine-tuned cp-decomposition. *arXiv preprint arXiv:1412.6553*, 2014. 2
- Y. LeCun, J. S. Denker, and S. A. Solla. Optimal brain damage. In *NeurIPS*, 1990. 1, 2, 3, 4, 7, 12
- Yann LeCun, Yoshua Bengio, and Geoffrey Hinton. Deep learning. *Nature*, 521(7553):436, 2015. 1
- Hao Li, Asim Kadav, Igor Durdanovic, Hanan Samet, and Hans Peter Graf. Pruning filters for efficient convnets. In *ICLR*, 2017. 1, 2, 3, 5, 8, 13
- Tuanhui Li, Baoyuan Wu, Yujie Yang, Yanbo Fan, Yong Zhang, and Wei Liu. Compressing convolutional neural networks via factorized convolutional filters. In *CVPR*, 2019. 8
- Lucas Liebenwein, Cenk Baykal, Harry Lang, Dan Feldman, and Daniela Rus. Provable filter pruning for efficient neural networks. In *ICLR*, 2020. 7, 8
- Mingbao Lin, Rongrong Ji, Yan Wang, Yichen Zhang, Baochang Zhang, Yonghong Tian, and Ling Shao. Hrank: Filter pruning using high-rank feature map. In *CVPR*, 2020a. 8
- Tao Lin, Sebastian U Stich, Luis Barba, Daniil Dmitriev, and Martin Jaggi. Dynamic model pruning with feedback. In *ICLR*, 2020b. 8
- Zhuang Liu, Jianguo Li, Zhiqiang Shen, Gao Huang, Shoumeng Yan, and Changshui Zhang. Learning efficient convolutional networks through network slimming. In *ICCV*, 2017. 1, 2
- Zhuang Liu, Mingjie Sun, Tinghui Zhou, Gao Huang, and Trevor Darrell. Rethinking the value of network pruning. In *ICLR*, 2019. 13
- Christos Louizos, Max Welling, and Diederik P Kingma. Learning sparse neural networks through l_0 regularization. In *ICLR*, 2018. 2
- James Martens and Roger Grosse. Optimizing neural networks with kronecker-factored approximate curvature. In *ICML*, 2015. 2
- Deepak Mittal, Shweta Bhardwaj, Mitesh M Khapra, and Balaraman Ravindran. Recovering from random pruning: On the plasticity of deep convolutional neural networks. In *WACV*, 2018. 6

-
- Dmitry Molchanov, Arsenii Ashukha, and Dmitry Vetrov. Variational dropout sparsifies deep neural networks. In *ICML, 2017a*. 8
- P. Molchanov, S. Tyree, and T. Karras. Pruning convolutional neural networks for resource efficient inference. In *ICLR, 2017b*. 1, 2
- Pavlo Molchanov, Arun Mallya, Stephen Tyree, Iuri Frosio, and Jan Kautz. Importance estimation for neural network pruning. In *CVPR, 2019*. 1, 2, 7, 8
- Michael C Mozer and Paul Smolensky. Skeletonization: A technique for trimming the fat from a network via relevance assessment. In *NeurIPS, 1989*. 1
- Adam Paszke, Sam Gross, Francisco Massa, Adam Lerer, James Bradbury, Gregory Chanan, Trevor Killeen, Zeming Lin, Natalia Gimelshein, Luca Antiga, et al. Pytorch: An imperative style, high-performance deep learning library. In *NeurIPS, 2019*. 5
- Hanyu Peng, Jiaxiang Wu, Shifeng Chen, and Junzhou Huang. Collaborative channel pruning for deep networks. In *ICML, 2019*. 8
- Mohammad Rastegari, Vicente Ordonez, Joseph Redmon, and Ali Farhadi. Xnor-net: Imagenet classification using binary convolutional neural networks. In *ECCV, 2016*. 2
- R. Reed. Pruning algorithms – a survey. *IEEE Transactions on Neural Networks*, 4(5):740–747, 1993. 1, 2
- Mark Sandler, Andrew Howard, Menglong Zhu, Andrey Zhmoginov, and Liang-Chieh Chen. Mobilenetv2: Inverted residuals and linear bottlenecks. In *CVPR, 2018*. 3
- Jürgen Schmidhuber. Deep learning in neural networks: An overview. *Neural networks*, 61:85–117, 2015. 1
- Karen Simonyan and Andrew Zisserman. Very deep convolutional networks for large-scale image recognition. In *ICLR, 2015*. 5
- Sidak Pal Singh and Dan Alistarh. Woodfisher: Efficient second-order approximations for model compression. *arXiv preprint arXiv:2004.14340*, 2020. 1, 2, 4, 8, 12
- Gilbert Strang. *Calculus*. Wellesley-Cambridge Press, 1991. 4
- Mingxing Tan and Quoc Le. Efficientnet: Rethinking model scaling for convolutional neural networks. In *ICML, 2019*. 3
- Chaoqi Wang, Roger Grosse, Sanja Fidler, and Guodong Zhang. Eigendamage: Structured pruning in the kronecker-factored eigenbasis. In *ICML, 2019a*. 1, 2, 4, 6, 7
- Huan Wang, Qiming Zhang, Yuehai Wang, and Haoji Hu. Structured probabilistic pruning for convolutional neural network acceleration. In *BMVC, 2018*. 7
- Huan Wang, Qiming Zhang, Yuehai Wang, Lu Yu, and Haoji Hu. Structured pruning for efficient convnets via incremental regularization. In *IJCNN, 2019b*. 2, 3
- Wei Wen, Chunpeng Wu, Yandan Wang, Yiran Chen, and Hai Li. Learning structured sparsity in deep neural networks. In *NeurIPS, 2016*. 1, 2, 7, 12
- Jianbo Ye, Xin Lu, Zhe Lin, and James Z Wang. Rethinking the smaller-norm-less-informative assumption in channel pruning of convolution layers. In *ICLR, 2018*. 2
- Ming Yuan and Yi Lin. Model selection and estimation in regression with grouped variables. *Journal of the Royal Statistical Society*, 68(1):49–67, 2006. 2
- Xiangyu Zhang, Jianhua Zou, Xiang Ming, Kaiming He, and Jian Sun. Efficient and accurate approximations of nonlinear convolutional networks. In *CVPR, 2015*. 2
- Xiangyu Zhang, Xinyu Zhou, Mengxiao Lin, and Jian Sun. Shufflenet: An extremely efficient convolutional neural network for mobile devices. In *CVPR, 2018*. 3

Zhuangwei Zhuang, Mingkui Tan, Bohan Zhuang, Jing Liu, Yong Guo, Qingyao Wu, Junzhou Huang, and Jinhui Zhu. Discrimination-aware channel pruning for deep neural networks. In *NeurIPS*, 2018. 8

Barret Zoph and Quoc Le. Neural architecture search with reinforcement learning. In *ICLR*, 2017. 3

A APPENDIX

A.1 EXPERIMENTAL SETTING DETAILS

Training setting summary. About the networks evaluated, we intentionally avoid AlexNet and VGG on the ImageNet benchmark because the single-branch architecture is no longer representative of the modern deep network architectures with residuals (but still keep VGG19 on the CIFAR analysis to make sure the findings are not limited to one specific architecture). Apart from some key settings stated in the paper, a more detailed training setting summary is shown as Tab. 5.

Table 5: Training setting summary. For the SGD solver, in the parentheses are the momentum and weight decay. For ImageNet, batch size 64 is used for pruning instead of the standard 256, which is because we want to save the training time.

| Dataset | CIFAR | ImageNet |
|------------------------|---------------------------------------|--|
| Solver | SGD (0.9, 5e-4) | SGD (0.9, 1e-4) |
| LR policy (prune) | Fixed (1e-3) | |
| LR policy (finetune) | Multi-step (0:1e-2, 60:1e-3, 90:1e-4) | Multi-step (0:1e-2, 30:1e-3, 60:1e-4, 75:1e-5) |
| Total epoch (finetune) | 120 | 90 |
| Batch size (prune) | 256 | 64 |
| Batch size (finetune) | 256 | |

Pruning ratios. Although several recent methods [Ding et al. \(2019b\)](#); [Singh & Alistarh \(2020\)](#) can automatically decide pruning ratios, in this paper we opt to consider pruning *independent* with the pruning ratio choosing. The main consideration is that pruning ratio is broadly believed to reflect the redundancy of different layers [LeCun et al. \(1990\)](#); [Wen et al. \(2016\)](#); [He et al. \(2017\)](#), which is an *inherent characteristic of the model*, thus should not be coupled with the subsequent pruning algorithms.

Before we list the specific pruning ratios, we explain how we set them. **(1)** For a ResNet, if it has N stages, we will use a list of N floats to represent its pruning ratios for the N stages. For example, ResNet56 has 4 stages in conv layers, then “[0, 0.5, 0.5, 0.5]” means “for the first stage (which is also the first conv layer), the pruning ratio is 0; the other three stages have pruning ratio of 0.5”. Besides, since we do not prune the last conv in a residual block, which means for a two-layer residual block (for ResNet56), we only prune the first layer; for a three-layer bottleneck block (for ResNet34 and 50), we only prune the first and second layers. **(2)** For VGG19, we use the following pruning ratio setting. For example, “[0:0, 1-9:0.3, 10-15:0.5]” means “for the first layer (index starting from 0), the pruning ratio is 0; for layer 1 to 9, the pruning ratio is 0.3; for layer 10 to 15, the pruning ratio is 0.5”.

With these, the specific pruning ratio for each of our experiments in the paper are listed in Tab. 6. We do not have strong rules to set them, except one, which is setting the pruning ratios of *higher* stages *smaller*, because the FLOPs of higher layers are relatively smaller (due to the fact that the spatial feature map sizes are smaller) and we are targeting more acceleration than compression. Of course, this scheme only is quite crude, yet as our results (Tab. 3 and 4) show, even with these crude settings, the performances are still competitive.

B PROOF OF EQ. 5

When a quadratic function \mathcal{E} converges at \mathbf{w}^* with Hessian matrix \mathbf{H} , it can be formulated as

$$\mathcal{E} = (\mathbf{w} - \mathbf{w}^*)^T \mathbf{H} (\mathbf{w} - \mathbf{w}^*) + C, \tag{10}$$

Table 6: Pruning ratio summary.

| Dataset | Network | Speedup | Pruned top-1 accuracy (%) | Pruning ratio |
|----------|----------|---------|---------------------------|-----------------------------|
| CIFAR10 | ResNet56 | 2.55× | 93.36 | [0, 0.75, 0.75, 0.32] |
| CIFAR100 | VGG19 | 8.84× | 67.56 | [0:0, 1-15:0.70] |
| ImageNet | ResNet34 | 1.32× | 73.44 | [0, 0.50, 0.60, 0.40, 0]* |
| ImageNet | ResNet50 | 1.49× | 76.24 | [0, 0.30, 0.30, 0.30, 0.14] |
| ImageNet | ResNet50 | 2.31× | 75.16 | [0, 0.60, 0.60, 0.60, 0.21] |
| ImageNet | ResNet50 | 2.56× | 74.75 | [0, 0.74, 0.74, 0.60, 0.21] |
| ImageNet | ResNet50 | 3.06× | 73.50 | [0, 0.68, 0.68, 0.68, 0.50] |

* In addition to the pruning ratios, several layers are skipped, following the setting of L_1 (pruned-B) Li et al. (2017). Specifically, we refer to the implementation of Liu et al. (2019) at <https://github.com/Erasmus-jie/rethinking-network-pruning/tree/master/imagenet/l1-norm-pruning>.

where C is a constant. Now a new function is made by increasing the L_2 penalty by small amount $\delta\lambda$, namely,

$$\hat{\mathcal{E}} = \mathcal{E} + \delta\lambda \mathbf{w}^T \mathbf{I} \mathbf{w}. \quad (11)$$

Let the new converged values be $\hat{\mathbf{w}}^*$, then similar to Eq. 10, $\hat{\mathcal{E}}$ can be formulated as

$$\hat{\mathcal{E}} = (\mathbf{w} - \hat{\mathbf{w}}^*)^T \hat{\mathbf{H}} (\mathbf{w} - \hat{\mathbf{w}}^*) + \hat{C}, \text{ where } \hat{\mathbf{H}} = \mathbf{H} + \delta\lambda \mathbf{I}. \quad (12)$$

Meanwhile, combine Eq. 10 and Eq. 11, we can obtain

$$\hat{\mathcal{E}} = (\mathbf{w} - \mathbf{w}^*)^T \mathbf{H} (\mathbf{w} - \mathbf{w}^*) + \delta\lambda \mathbf{w}^T \mathbf{I} \mathbf{w} + C. \quad (13)$$

Compare Eq. 13 with Eq. 12, we have

$$(\mathbf{H} + \delta\lambda \mathbf{I}) \hat{\mathbf{w}}^* = \mathbf{H} \mathbf{w}^* \Rightarrow \hat{\mathbf{w}}^* = (\mathbf{H} + \delta\lambda \mathbf{I})^{-1} \mathbf{H} \mathbf{w}^*. \quad (14)$$

C PROOF OF EQ. 7

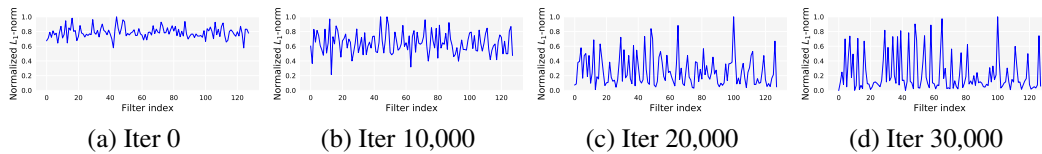
$$\hat{\mathbf{H}} = \begin{Bmatrix} h_{11} + \delta\lambda & h_{12} \\ h_{12} & h_{22} + \delta\lambda \end{Bmatrix} \Rightarrow \hat{\mathbf{H}}^{-1} = \frac{1}{|\hat{\mathbf{H}}|} \begin{Bmatrix} h_{22} + \delta\lambda & -h_{12} \\ -h_{12} & h_{11} + \delta\lambda \end{Bmatrix} \quad (15)$$

Therefore, $\hat{\mathbf{w}}^* = \hat{\mathbf{H}}^{-1} \mathbf{H} \mathbf{w}^* \Rightarrow$

$$\begin{aligned} \begin{Bmatrix} \hat{w}_1^* \\ \hat{w}_2^* \end{Bmatrix} &= \hat{\mathbf{H}}^{-1} \mathbf{H} \begin{Bmatrix} w_1^* \\ w_2^* \end{Bmatrix} = \frac{1}{|\hat{\mathbf{H}}|} \begin{Bmatrix} h_{22} + \delta\lambda & -h_{12} \\ -h_{12} & h_{11} + \delta\lambda \end{Bmatrix} \begin{Bmatrix} h_{11} & h_{12} \\ h_{12} & h_{22} \end{Bmatrix} \begin{Bmatrix} w_1^* \\ w_2^* \end{Bmatrix} \\ &= \frac{1}{|\hat{\mathbf{H}}|} \begin{Bmatrix} (h_{11}h_{22} + h_{11}\delta\lambda - h_{12}^2)w_1^* + \delta\lambda h_{12}w_2^* \\ (h_{11}h_{22} + h_{22}\delta\lambda - h_{12}^2)w_2^* + \delta\lambda h_{12}w_1^* \end{Bmatrix}. \end{aligned} \quad (16)$$

D FILTER L_1 -NORM CHANGE OF VGG19

In Fig. 1 (Row 2), we plot the filter L_1 -norm change over time for ResNet50 on ImageNet. Here we plot the case of VGG19 on CIFAR100 to show the weight separation phenomenon under growing regularization is a *general* one across different datasets and networks.

Figure 2: Normalized filter L_1 -norm over iterations for VGG19 layer3.

E HYPER-PARAMETERS AND SENSITIVITY ANALYSIS

There are five introduced values in our methods: regularization ceiling τ , ceiling for picking τ' , interval K_u, K_s , granularity $\delta\lambda$. Their settings are summarized in Tab. 7. Among them, the ceilings are set through validation: $\tau = 1$ is set to make sure the unimportant weights are pushed down enough (as stated in the main paper, normally after the regularization training, their magnitudes are too small to cause significant accuracy degradation if they are completely removed). $\tau' = 0.01$ is set generally for the same goal as τ , but since it is applied to *all* the weight (not just the unimportant ones), we only expect it to be moderately large (thus smaller than τ) so that the important and unimportant can be differentiated with a clear boundary. For the $\delta\lambda$, we use a very *small* regularization granularity $\delta\lambda$, which our theoretical analysis is based on. We set its value to $1e-4$ for GReg-1 and $1e-5$ for GReg-2 with reference to the original weight decay value 5×10^{-4} (for CIFAR models) and 10^{-4} (for ImageNet models). Note that, these values come from our methods per se, not directly related to datasets and networks, thus are invariant to them. This is why we can employ the same setting of these three hyper-parameters in *all* our experiments, freeing practitioners from heavy tuning when dealing with different networks or datasets.

Table 7: Hyper-parameters of our methods.

| Notation | Default value (CIFAR) | Default value (ImageNet) |
|-----------------|---------------------------------|--------------------------|
| $\delta\lambda$ | GReg-1: $1e-4$, GReg-2: $1e-5$ | |
| τ | 1 | |
| τ' | 0.01 | |
| K_u | 10 iterations | 5 iterations |
| K_s | 5k iterations | 40k iterations |

A little bit of change is for K_u, K_s . Both are generally to let the network have enough time to converge to the new equilibrium. Generally, we prefer large update intervals, yet we also need to consider the time complexity: Too large of them will bring too many iterations, which may be unnecessary. Among them, K_s is less important since it is to stabilize the large regularization ($\tau = 1$). We introduce it simply to make sure the training is fully converged. Therefore, the possibly more sensitive hyper-parameter is the K_u (set to 5 for ImageNet and 10 for CIFAR). Here we will show the performance is insensitive to the varying K_u . As shown in Tab. 8, the peak performance appears at around $K_u = 15$ for ResNet56 and $K_u = 10$ for VGG19. We simply adopt 10 for a uniform setting in our paper. We did not heavily tune these hyper-parameters, yet as seen, they work pretty well across different networks and datasets. Notably, even for the *worst* cases in Tab. 8 (in blue color), they are still significantly better than those of the “ L_1 +one-shot” scheme, demonstrating the robustness of the proposed algorithm.

Table 8: Sensitivity analysis of K_u on CIFAR10/100 datasets with the proposed GReg-1 algorithm. $K_u = 10$ is the default setting. Pruning ratio 90% (ResNet56) and 70% (VGG19) are explored here. Experiments are randomly run for 3 times with mean accuracy and standard deviation reported. **The best** is highlighted with **bold** and **the worst** is highlighted with **blue color**.

| K_u | 1 | 5 | 10 | 15 | 20 | L_1 +one-shot |
|---------------------|------------------|----------------------------------|----------------------------------|----------------------------------|----------------------------------|------------------|
| Acc. (% , ResNet56) | 89.40 \pm 0.04 | 89.38\pm0.13 | 89.49 \pm 0.23 | 89.69\pm0.05 | 89.62 \pm 0.13 | 87.34 \pm 0.21 |
| Acc. (% , VGG19) | 67.22 \pm 0.33 | 67.32 \pm 0.24 | 67.35\pm0.15 | 67.06 \pm 0.40 | 66.93\pm0.22 | 66.05 \pm 0.04 |

F MORE RESULTS OF PRUNING SCHEDULE COMPARISON

In Tab. 1, we show using L_1 -norm sorting, our proposed GReg-1 can consistently surpass the one-shot schedule even pruning the same weights. Here we ask a more general question: Can the benefits from a regularization-based schedule consistently appear, *agnostic to the weight importance scoring criterion*? This question is important because it will show if the gain from a better pruning schedule is only a bonus concurrent with the L_1 criterion or a really universal phenomenon. Since there are literally so many weight importance criteria, we cannot ablate them one by one. Nevertheless, given a pre-trained model and a pruning ratio r , no matter what criterion, its role is to select a filter *subset*.

For example, if there are 100 filters in a layer and $r = 0.5$, then they are at most $\binom{100}{50}$ importance criteria in theory for this layer. We can simply *randomly* pick a subset of filters (which corresponds to certain criterion, albeit unknown) and compare the one-shot way with regularization-based way on the subset. Based on this idea, we conduct five random runs on the ResNet56 and VGG19 to explore this. The pruning ratio is chosen as 90% for ResNet56 and 70% for VGG19 because under this ratio the compression (or acceleration) ratio is about 10 times, neither too large nor too small (where the network can heal itself regardless of pruning methods).

The results are shown in Tab. 9. Here is a sanity check: Compared with Tab. 1, the mean accuracy of pruning randomly picked filters should be *less* than pruning those picked by L_1 -norm, confirmed by 86.85% vs. 87.34% for ResNet56 and 65.04% vs. 66.05% for VGG19. As seen, in each run, the regularization-based way also *significantly* surpasses its one-shot counterpart. Although five random runs are still too few given the exploding potential combinations, yet as shown by the accuracy standard deviations, the results are quite stable and thus qualified to support our finding that the regularization-based pruning schedule is better to the one-shot counterpart.

Table 9: Comparison between pruning schedules: one-shot vs. GReg-1. Pruning ratio is 90% for ResNet56 and 70% for VGG19. In each run, the weights to prune are picked *randomly* before the training starts.

| ResNet56 + CIFAR10 | Run #1 | Run #2 | Run #3 | Run #4 | Run #5 | Mean \pm std |
|---------------------------|--------------|--------------|--------------|--------------|--------------|----------------------------------|
| Acc. (% , one-shot) | 87.57 | 87.00 | 86.27 | 86.75 | 86.67 | 86.85 \pm 0.43 |
| Acc. (% , GReg-1, ours) | 89.26 | 88.98 | 88.78 | 89.42 | 88.96 | 89.08\pm0.23 |
| VGG19 + CIFAR100 | Run #1 | Run #2 | Run #3 | Run #4 | Run #5 | Mean \pm std |
| Acc. (% , one-shot) | 64.56 | 65.06 | 65.07 | 65.05 | 65.48 | 65.04 \pm 0.29 |
| Acc. (% , GReg-1, ours) | 66.63 | 66.57 | 66.80 | 66.80 | 67.16 | 66.79\pm0.21 |